SCIENCE CHINA
Technological Sciences

March 2010 Vol.53 No.3: 776–781
doi: 10.1007/s11431-009-0384-x

Influence of Zn ion implantation on structures and field emission properties of multi-walled carbon nanotube arrays

CHEN KeFan, DENG JianHua, ZHAO Fei, CHENG GuoAn* & ZHENG RuiTing

Key Laboratory of Beam Technology and Material Modification of Ministry of Education, College of Nuclear Science and Technology, Beijing Normal University, Beijing100875, China

Received May 28, 2009; accepted August 5, 2009

The structures and field emission properties of multi-walled carbon nanotube arrays implanted with Zn^+ by MEVVA ion implanter have been investigated. The results revealed that Zn^+ implantation induced structural damage and that the top of carbon nanotubes with multi-layered graphite structure were transformed into carbon nanowires with amorphous structure. Meanwhile, C: Zn solid solution was synthesized after Zn^+ implantation. The turn-on field and threshold field were 0.80 and 1.31 V/μm, respectively for original multi-walled carbon nanotube arrays and were reduced to 0.66 and 1.04 V/μm due to the synthesis of C and Zn composite, in which the work function was reduced after low doses of Zn^+ implantation. It is indicated that low doses of Zn^+ implantation can improve field emission performance of multi-walled carbon nanotube arrays. Otherwise, high doses of Zn^+ implantation can reduce field emission properties of multi-walled carbon nanotube arrays, because radiation damage reduces the electric field enhancement factor.

multi-walled carbon nanotubes, ion implantation, field electron emission

Citation: Chen K F, Deng J H, Zhao F, et al. Influence of Zn ion implantation on the structures and field emission properties of multi-walled carbon nanotube arrays. Sci China Tech Sci, 2010, 53: 776–781, doi: 10.1007/s11431-009-0384-x

In 1991, Iijima firstly synthesized carbon nanotubes (CNTs) [1] in direct current arc discharge experiment, whose diameters were from a few nanometers to tens nm and whose lengths were from tens nm to a micron. Subsequent studies [2–4] found that CNTs had a unique structure and excellent physical and chemical properties. Their tremendous application prospect has aroused wide interest.

Field electron emission is one of the important potential applications of CNTs. Rinzler firstly reported the field emission characteristics of a single multi-walled carbon nanotube and pointed out that it had a very low threshold field and high field emission current density [5]. The study of Cheng et al. [6] showed that the electrons emitted from the top of CNTs.

Doping can change the structure of CNT emitters and improve the field emission properties of CNTs. Some research groups have synthesized nitrogen, boron or silicon doped carbon nanotubes [7–10]. Nitrogen-doped carbon nanotube arrays prepared by Chai et al. [11] have a low turn-on field (1.60 V/μm) and high density of emission sites. Liu et al. [12] found that gallium-doping introduced the formation of new states near the Fermi level in CNTs, and reduced the work function and enhanced the density of electron emission. Some reports [13, 14] found that Cs-doped single-walled carbon nanotubes should reduce their work function and increase the field emission current density. Scholars found that titanium carbon compounds synthesized by deposition of titanium films on the surface of CNTs had lower work function, which improved the field emission properties of CNTs [15].

In this paper, multi-walled carbon nanotube arrays with high density and good orientation were prepared by thermal

*Corresponding author (email: gacheng@bnu.edu.cn)

chemical vapor deposition and then implanted with energetic Zn^+ by using of MEVVA (metal vapor vacuum arc) [16] ion implanter. The synthesis and the field emission properties of C: Zn solid solution nanowires were investigated.

1 Experimental details

MWCNT arrays were synthesized by thermal chemical vapor deposition method. Firstly, 5 nm Fe films used as catalyst were deposited on silicon substrate by magnetron sputtering method. Secondly, the sample was placed in a quartz tube furnace. N_2 gas was passed to clean the pipe for about 20 min, and then converted to H_2 gas to start heating up. Thirdly, when the temperature reached 750°C, C_2H_2 was passed to grow carbon nanotubes. The purity of the gases used in the work was better than 99.9%.

Zn ion doping was carried out on the MEVVA ion implanter. The average energy of Zn^+ was aout 54 keV. The average beam density was 0.127 μA/mm^2. The Zn doped doses were in the range from 1×10^{16} to 2×10^{17} ions/cm^2 and the angle of ion incidence was about 45º. The ion range and average displacement of atom per implanting ion were calculated by TRIM-1996.

Scanning electron microscopy (JSM-4800, SEM), high-resolution transmission electron microscopy (TECNAI F30, TEM), X-ray photoelectron spectroscopy (PHI Quantera SXM, XPS) and field emission measurement system were employed to characterize morphology, chemical state and field emission properties of the WMCNTs. The field emission measurements of samples with area from 0.03 to 0.10 cm^2 were carried out in the bipolar measurement equipment at room temperature, in which measurement distance was about 2362 μm, and base pressure of chamber was about 1×10^{-7} Pa. Applied voltage was 0–3500 V. Voltage regulation rate was 500 V/min. The measurement data could be automatically recorded by a computer connected to the measurement system.

2 Results and discussion

2.1 The morphology of Zn-dopped multi-walled carbon nanotube arrays

SEM images (cross-section view) of carbon nanotube arrays with different doses of Zn^+ implantation are shown in Figure 1 and the top view ones are shown in Figure 2. When the doses is less than 6×10^{16} ions/cm^2, the morphology changes in the top of carbon nanotubes is small and the micro-structure maintains the original form of the carbon nanotubes. As the implantation dose increases, the deformation and adhesion of the top of carbon nanotubes become apparent, the diameter of carbon nanotubes increases, tubular morphology becomes blurred and structural damage becomes clear. This is because low doses of Zn^+ implantation cause small structural damage, while large doses cause large structural damage.

The ion radiation damage of WMCNTs with different Zn ion doping doses can be evaluated by the displacement per atom (dpa), which is calculated by TRIM-1996 simulation program. The calculation formula of dpa is as follows

$$\mathrm{dpa} = \frac{\Phi \cdot N_1}{N \cdot l}, \tag{1}$$

where Φ is ion dose (cm^{-2}), N_1 is the average displacement of carbon atom per implanting ion, N is the atomic density (atoms/cm^3) of target and l is the depth of ion implantation (cm). TRIM simulation results shows that when the average energy of Zn^+ is 54 keV, the average displacement of car-

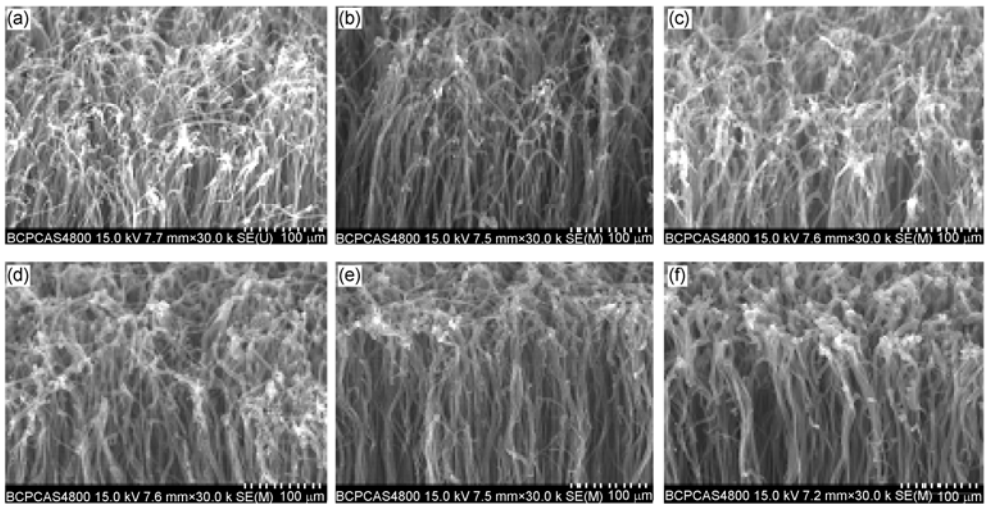

Figure 1 SEM images (cross-section view) of carbon nanotube arrays with different doses of Zn^+ implantation. (a) Original; (b) 1×10^{16} ions/cm^2; (c) 3×10^{16} ions/cm^2; (d) 6×10^{16} ions/cm^2; (e) 1×10^{17} ions/cm^2; (f) 2×10^{17} ions/cm^2.

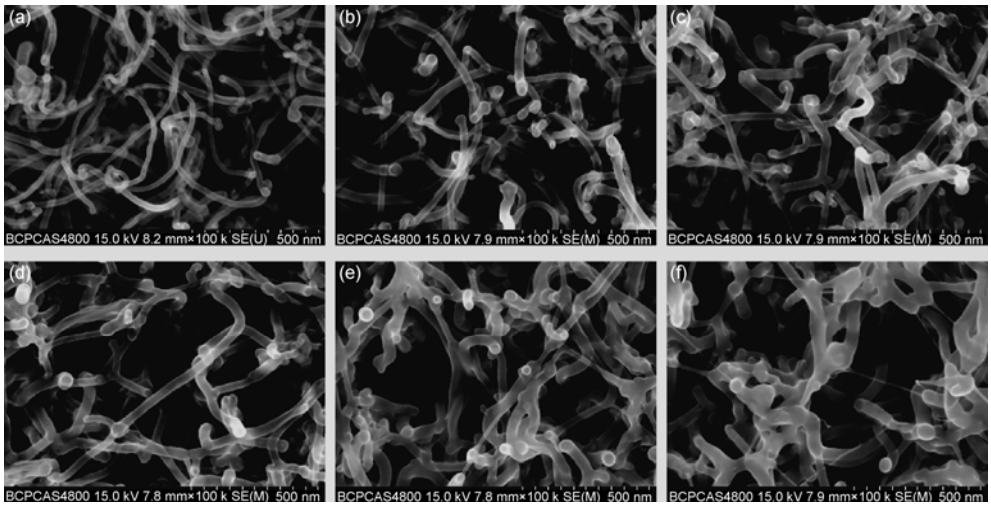

Figure 2 SEM images (top view) of carbon nanotube arrays with different doses of Zn^+ implantation. (a) Original; (b) 1×10^{16} ions/cm^2; (c) 3×10^{16} ions/cm^2; (d) 6×10^{16} ions/cm^2; (e) 1×10^{17} ions/cm^2; (f) 2×10^{17} ions/cm^2.

bon atom per implanting ion (N_1) is 373 atoms/ion. The depth of Zn^+ implantation (l) is about 4 μm which is measured by the EDX analysis of multi-walled carbon nanotube arrays. So we can calculate the dpas of different doses of Zn^+ implantation as shown in Table 1.

From Table 1，it can be seen that when the dose is less than 6×10^{16} ions/cm^2, the dpa is less than 1. This means that the ion radiation damage and the influence of Zn-doping on microstructure of WMCNTs are small. However, when the dose is more than 1×10^{17} ions/cm^2, the dpa is larger than 1, which means the ion radiation damage and the influence of Zn-doping on microstructure of WMCNTs are large. The changes of dpa in TRIM simulation results with different doses are consistent with the changes of SEM morphology analysis.

Figure 3 shows the HRTEM images of multi-walled carbon nanotubes with Zn^+ implantation. For the range of CNT without Zn^+ implantation (shown in Figure 3(a)), a clear graphite tubular structure with multi-layer can be observed. In the near tip of the carbon nanotubes, multi-layer structure of carbon nanotube has transformed into amorphous carbon nanowires and diameter of amorphous carbon nanowires is larger than that of the carbon nanotube due to large ion radiation damage (see Figure 3(c)). The diameter increasing of carbon nanowires is due to the formation of a large number of vacancies and interstitial atoms and part of graphite layer curvedness. In the transition area between Figures 3(a) and (c), whose Zn^+ implantation dose is less than Figure 3(c)'s, the high resolution TEM image shows graphite tubular structure with multi-layer in which partial structure damage is observed (see Figure 3(b)). Figure 3(d) is a high resolution image in the head of carbon nanowires with hemisphere structure whose ion radiation damage is the largest and the distribution of carbon atoms is out-of order, which means the formation of amorphous structure. Besides, the EDX analysis of this part proves the existence of Zn element except C element. So, according to HRTEM images and EDX analysis, C: Zn amorphous solid solution in nanowires is formed after Zn^+ implantation.

Table 1 The dpa of WMCNTs implanted with different Zn ion doses

Dose (cm^{-2})	1×10^{16}	3×10^{16}	6×10^{16}	1×10^{17}	2×10^{17}
dpa	0.13	0.40	0.80	1.33	2.66

2.2 The chemical state of elements in Zn-dopped multi-walled carbon nanotube arrays

In order to further understand the chemical structures of C and Zn in the complex nanowires, X-ray photoelectron spectroscopy was used to analyze the chemical states of C and of Zn. Figure 4(a) shows C1s XPS line of CNTs implanted by Zn ions with 3×10^{16} ions/cm^2 dose. C1s XPS spectrum line has been decomposed to three peaks (284.1, 285.9 and 288 eV), corresponding to graphite carbon [17] which has the strongest peak and two kinds of organic pollution carbons [18, 19]. This shows that Zn^+ implantation dose not change the chemical states of C and the main structure is similar to graphite. Zn2p3 XPS spectrum line is composed of only peak (1021.7 eV), corresponding to simple substance of Zn [20] (as shown in Figure 4(b)). It is demonstrated that there is no formation of C/Zn compound during ion implantation. According to that, it can be confirmed that C: Zn solid solution in carbon nanowires is formed after Zn^+ implantation. At the same time, the increase of intensity for Zn2p3 spectrum line with the increasing of the Zn^+ implantation dose indicates that the content of Zn in solid solution nanowires increases.

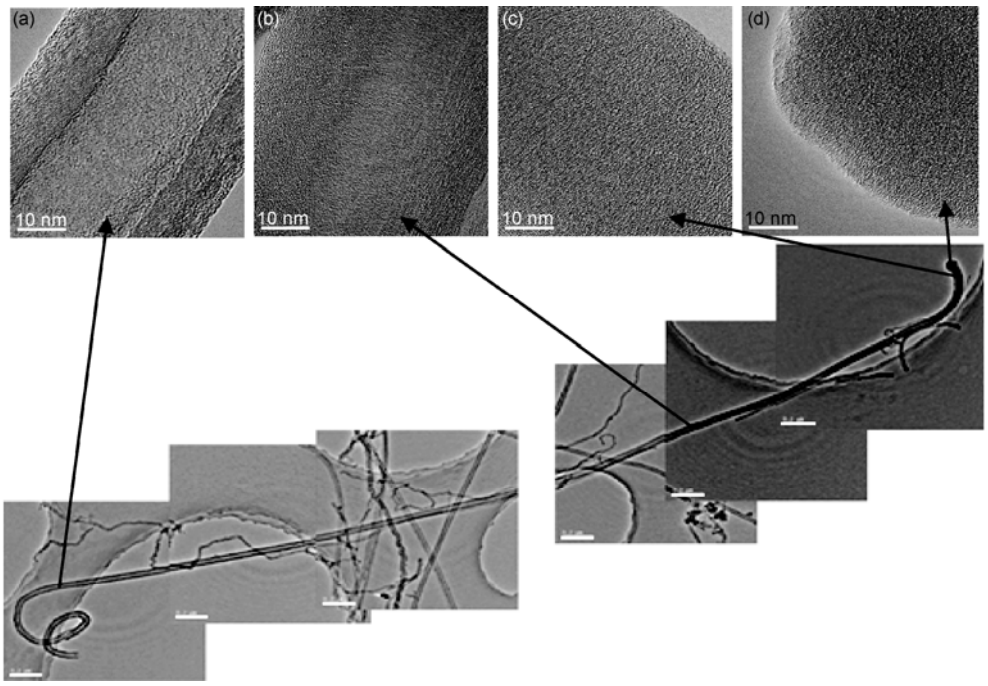

Figure 3 HRTEM images of carbon nanotubes with Zn^+ implantation.

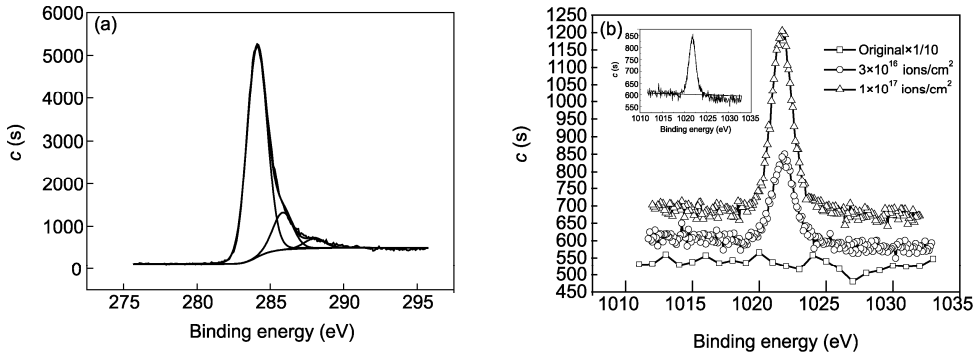

Figure 4 (a) C1s XPS line and sub-peaks with 3×10^{16} ions/cm^2 dose of Zn^+ implantation; (b) Zn2p3 XPS line with different Zn^+ implantation doses. The inset in (b): Zn2p3 XPS line with 3×10^{16} ions/cm^2 dose of Zn^+ implantation.

2.3 Influence of Zn^+ implantation on the field emission properties of multi-walled carbon nanotube arrays

Figure 5(a) shows field emission characteristics of carbon nanotube arrays implanted with different doses. It can be seen that the *J*-*E* curves move to the low field when the Zn^+ implantation dose increases from zero to 6×10^{16} ions/cm^2. This means that field emission properties of carbon nanotube array are gradually improved during low dose implantation. On the other hand, the *J*-*E* curves move to the high field when the Zn^+ implantation dose increases from 6×10^{16} to 2×10^{17} ions/cm^2, which means that field emission properties are reduced. The approximate linear relationships between ln(*J*/*E*–2) and 1/*E* in *F*-*N* plots at high current density area proves that the data in Figure 5(a) are field induced electron emission.

The turn-on field and threshold field of carbon nanotube arrays implanted with different Zn^+ implantation doses are shown in Figure 6. It can be seen that the turn-on field decreases from 0.80 to 0.66 V/μm (the dose is 3×10^{16} ions/cm^2), and the threshold field reduces from 1.31 to 1.04 V/μm (the dose is 3×10^{16} ions/cm^2) when the Zn^+ implantation dose increases from 0 to 6×10^{16} ions/cm^2. After that, the turn-on field and threshold field gradually rise when the Zn^+ implantation dose increases from 6×10^{16} to 2×10^{17} ions/cm^2. This shows that low dose Zn^+ implantation can improve field emission performance of multi-walled carbon nanotube arrays and reduce the turn-on field and threshold field.

For the change of field emission properties of carbon nanotubes after Zn^+ implantation, there are two different stages. The first stage is from the original to 6×10^{16} ions/ cm^2

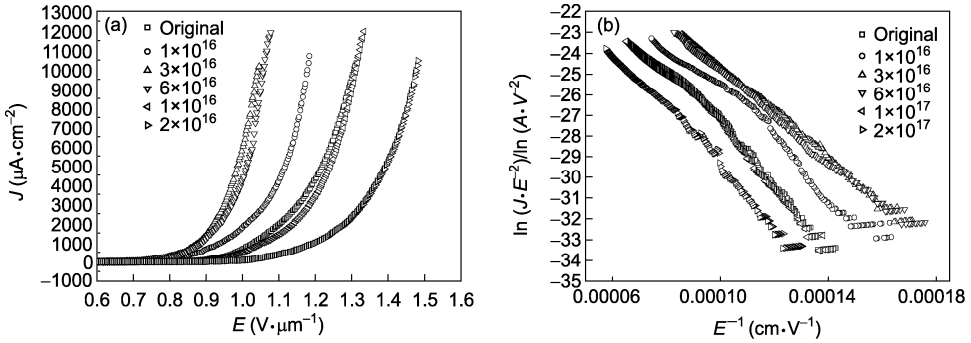

Figure 5 (a) *J-E* curves of carbon nanotube arrays implanted with different Zn^+ implantation doses; (b) the corresponding *F-N* plot.

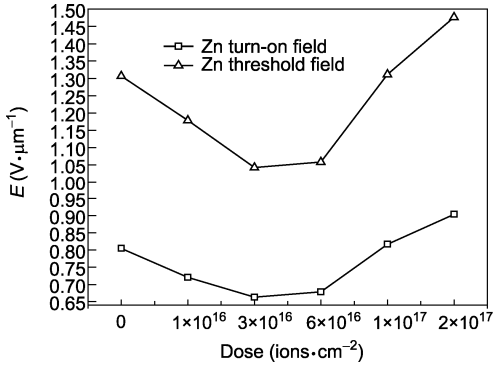

Figure 6 The turn-on field and threshold field of carbon nanotube arrays versus Zn^+ implantation dose.

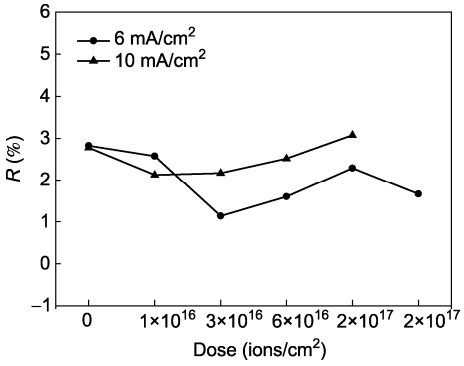

Figgure 7 The field emission stabilization of different doses Zn-doped multi-walled carbon nanotube arrays versus ion implantation dose.

Zn^+ implantation. It can be seen that the change in morphology of carbon nanotube arrays is relatively small from Figures 1 and 2, and the dpa is less than 1 in this stage. According to the impact factors [12] of field enhancement factor, the field enhancement factor is approximately unchanged and the effective work function of carbon nanotube arrays can be reduced from 4.59 [21] to 4.04 eV during Zn^+ implantation, to enhance the field emission properties in the first stage. This change is probably because the formation of C: Zn solid solution in carbon nanowires changes the electronic structure of carbon nanotubes. From the above, C: Zn solid solution in carbon nanowires shows excellent field emission characteristics.

The second stage is in the Zn^+ implantation range from 6×10^{16} to 2×10^{17} ions/cm^2. It can be seen that the change in morphology of carbon nanotube arrays is relatively large from Figures 1 and 2 and the dpa is more than 1 in this stage. The entwisted carbon nanotubes and the large particles in the top of array have been formed during high dose implantation. The structure damage reduces the number of the field electron emission points to induce the reducing of the field emission performance.

At the same time, the field emission stabilization of different doses Zn-doped multi-walled carbon nanotube arrays have been measured at different current densities. Figure 7 shows the ratio *R* between the standard deviation (SD) and the mean current density versus ion implantation dose.

From Figure 7, it can be seen that the Zn-doping dose has a high influence on the field emission stabilization of multi-walled carbon nanotube arrays. For the low dose implantation, the ratio *R* can be reduced from 2.8% to 2.1% at the current density of 6 mA/cm^2 and from 2.8% to 1.1% at the current density of 10 mA/cm^2. This means that Zn-doping at a lower dose can improve the field emission stabilization of multi-walled carbon nanotube arrays, but high dose Zn-doping will debase it.

3 Conclusions

(i) Energetic Zn ion implantation induces the structure amorphization of multi-layer carbon nanotube and the formation of C: Zn solid solution nanowire in which the diameter of carbon nanowires is larger than that of carbon nanotubes. High dose implantation destroys the array structure and induces the formation of entwisted carbon nanotubes in the top of arrays.

(ii) C: Zn solid solution nanowires which are formed after low dose Zn^+ implantation change the electronic structure of MWCNTs and has excellent field emission characteristics. For C: Zn solid solution nanowires, the minimum turn-on field and minimum threshold filed are 0.66 and 1.04 V/ μm, respectively. Otherwise, high doses Zn^+ implantation can reduce field emission properties of carbon nanotube arrays.

(iii) Low dose Zn-doping can improve the field emission stabilization of multi-walled carbon nanotube arrays, but high dose Zn-doping will debase it.

This work was supported by the National Basic Research Program of China ("973" Project)(Grant No. 2010CB832905), the National Natural Science Foundation of China (Grant No. 10575011) and the Key Scientific and Technological Project of Ministry of Education of China (Grant No. 108124).

1 Iijima S. Helical microtubes of graphitic carbon. Nature, 1991, 354: 56－58
2 Zheng R T, Cheng G A, Peng Y B, et al. Synthesis of vertically aligned carbon nanotube arrays on silicon substrates. Sci China Ser E-Tech Sci, 2004, 47(5): 616－624
3 Liu H P, Cheng G A, Zheng R T, et al. Layered growth of aligned carbon nanotubes arrays on silicon wafers. J Mol Catal A: Chem, 2006, 247: 52－57
4 Liu H P, Cheng G A, Zheng R T, et al. Effects of the restructuring of Fe catalyst films on chemical vapor deposition of carbon nanotubes. Surf Coat Technol, 2008, 202: 3157－3163
5 Rinzler A G, Hafner J H, NIkolaev P, et al. Unraveling nanotubes: Field emission from an atomic wire. Science, 1995, 269: 1550－1553
6 Cheng Y, Zhou O. Electron field emission from carbon nanotubes. C R Phys, 2004, 4: 1021－1033
7 Sharma R B, Late D J, Joag D S, et al. Field emission properties of boron and nitrogen doped carbon nanotubes. Chem Phys Lett, 2006, 428: 102－108
8 Yu J, Bai X D, Ahn J, et al. Highly oriented rich boron B-C-N nanotubes by bias-assisted hot filament chemical vapor depositon. Chem Phys Lett, 2000, 323: 529－533
9 Han W Q, Bando Y, Kurashima K, et al. Boron-doped carbon nanotubes prepared through a substitution reaction. Chem Phys Lett, 1999, 299: 368－373
10 Liu H P, Cheng G A, Liang C L, et al. Fabrication of silicon carbide nanowires/carbon nanotubes heterojunction arrays by high-flux Si ion implantation. Nanotechnol, 2008, 19: 245606(1-7)
11 Chai Y, Yu L G, Wang M S, et al. Fabrication of nitrogen-doped carbon nanotube arrays and their field emission properties. Acta Scientiarum Naturalium Universitatis Pekinensis, 2006, 42(1): 89－92
12 Liu K, Li H Y, Li Q, et al. Field emission properties of gallium-doped carbon nanotubes. J Henan Uni (Nat Sci), 2006, 36(4): 24－27
13 Suzu K S, Bower C, Watanabe Y, et al. Work functions and valence band states of pristine and Cs-intercalated single-walled carbon nanotube bundles. Appl Phys Lett, 2000, 76(26): 4007－4009
14 Wadhawan A, Stullcup R E, Perez J M.. Effects of Cs deposition of the field-emission properties of single-walled carbon-nanotube bundles. Appl Phys Lett, 2001, 78(1): 108－110
15 Qing Y X, Hu M. Characterization and field emission characteristics of carbon nanotubes modified by titanium carbide. Appl Surf Sci, 2008, 254(11): 3313－3317
16 Zhang T H, Wu Y G. Science and Application of Ion Beam Materials Modification. Beijing: Science Press, 1999
17 Bertoncello R, Casagrande A, Casarin M, et al. TiN, TiC and Ti(C, N) film characterization and its relationship to tribological behavior. Surf Interface Anal, 1992, 18: 525－531
18 Folkesson B, Sundverg P, Larsson R. On the core electron binding energy of carbon and the effective charge of the carbon atom. J Electron Spectrosc Relat Phenom, 1988, 46: 19－29
19 Rats D, Sevely J, Vandenbulcke L, et al. Characterization of diamond films deposited on titanium and its alloys. Thin Solid Films, 1995, 270: 177－183
20 Briggs D, Seah M P. Practical Surface Analysis. 2nd ed. New York: John Willey & Sons, 1993
21 Chen Z X, Cao G C, Zhang Q, et al. Fabrication of large current density carbon nanotuhe based field emitters. High Power Laser Part Beams, 2006, 18(12): 2070－2073